ACS Chemical Neuroscience

Research Article

pubs.acs.org/chemneuro

Aging Related Changes of Retina and Optic Nerve of *Uromastyx aegyptia* and *Falco tinnunculus*

Hassan I. H. El-Sayyad,*[,†] Soad A. Khalifa,[†] Asma S. AL-Gebaly,[‡] and Ahmed A. El-Mansy[†]

[†]Department of Zoology, Faculty of Science, Mansoura University, Mansoura 002050, Egypt

[‡]Department of Biology, Science College, Princess Noura Bint Abdul Rahman University, Riyadh 11421, Kingdom of Saudia Arabia

ABSTRACT: Aging is a biological phenomenon that involves gradual degradation of the structure and function of the retina and optic nerve. To our knowledge, little is known about the aging-related ocular cell loss in avian (*Falco tinnunculus*) and reptilian species (*Uromastyx aegyptia*). A selected 90 animals of pup, middle, and old age *U. aegyptia* (reptilian) and *F. tinnunculus* (avian) were used. The retinae and optic nerves were investigated by light and transmission electron microscopy (TEM) and assessments of neurotransmitters, antioxidant enzymes (catalase, superoxide dismustase and glutathione s transferase), caspase-3 and -7, malonadialdhyde, and DNA fragmentation. Light and TEM observations of the senile specimens revealed apparent deterioration of retinal cell layers, especially the pigmented epithelium and photoreceptor outer segments. Their inclusions of melanin were replaced by lipofuscins. Also, vacuolar degeneration and demyelination of the optic nerve axons were detected. Concomitantly, there was a marked increase of oxidative stress involved reduction of neurotransmitters and antioxidant enzymes and an increase of lipid peroxidation, caspase-3 and -7, subG0/G1 apoptosis, and P53. We conclude that aging showed an inverse relationship with the neurotransmitters and antioxidant enzymes and a linear relationship of caspases, malondialdhyde, DNA apoptosis, and P53 markers of cell death. These markers reflected the retinal cytological alterations and lipofuscin accumulation within inner segments.

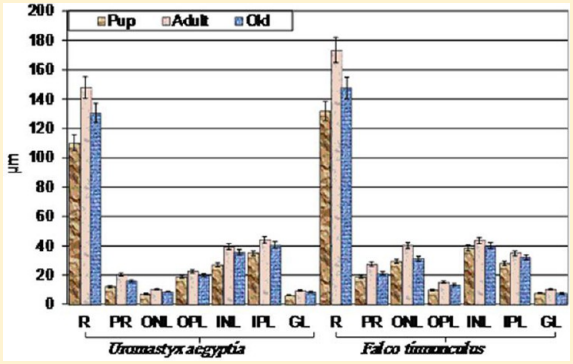

KEYWORDS: *Aging, retina, optic nerve, Falco tinnunculus, Uromastyx aegyptia*

Aging is a complex biological phenomenon that depends upon the interaction of numerous genes, cellular pathways, and environmental risk factors. It leads to a gradual deterioration of physiological function, including impairment of vision and deterioration of the retinal cells.[1]

Age-related macular degeneration (AMD) and cataracts are the most frequent eye disorders in elderly people worldwide.[2] AMD is characterized by progressive degeneration of the retinal pigmented epithelium, and choroids that impair vision.[3,4] Experimental OXYS rats[5,6] and other rat models[7,8] were found to develop retinal damage with clinical, morphological, and molecular features similar to those in human AMD.

The retinal cells encounter a cumulative amount of oxidative and metabolic stress that may be a universal feature of the aging process. Increased oxidative stress leads to the dysfunction of various metabolic and signaling pathways. The photoreceptor membranes are rich in polyunsaturated fatty acids and are more sensitive to damage.[9,10]

The avian eye resembles that of a reptile, with ciliary muscles that can change the shape of the lens rapidly and to a greater extent than in mammals. Recently, birds have become an important part of veterinary ophthalmology consultations due to an increasing awareness of the environment and the conservation of nature and its species. Good vision is especially important in birds due to the direct influence on flight, feeding, and breeding. Compared to the mammalian eye, the avian eye varies in size, voluntary contraction of the pupil, ossicles in the sclera, avascular retina, and the presence of the pecten protruding into the vitreous chamber.[11]

The studied avian (*Falco tinnunculus*) and reptilian (*Uromastyx aegyptia*) species are diurnal. Their distal end of the cone inner segment contains a colored oil droplet, which contains high concentrations of carotenoids, localized through which light passes before reaching the visual pigment. They act as filters, removing some wavelengths and narrowing the absorption spectra of the pigments, reducing the response overlap between pigments and increasing the number of colors.[12,13]

Aging patterns in the wild are predominantly documented in birds and mammals,[14] and very little is known in other taxa.[15] Reptiles have been the subject of few studies,[16,17] and these do not provide enough evidence for generalization. The process may be either a genetic drift caused by decreased evolutionary pressure at later ages or mutation accumulation or antagonistic pleiotropy and so forth. Indeterminately growing reptiles are prime candidates for aging research.[16]

Received: August 22, 2013
Revised: October 19, 2013
Published: November 11, 2013

There are three true individual aging processes not related to the selective appearance or disappearance of individuals in populations: maturation, terminal investment, and senescence.[17] The cone photoreceptors of many vertebrates, including birds, turtles, and lizards, showed colored-oil droplets which decrease cone quantum catch and reduce the overlap in sensitivity between spectrally adjacent cones[18] and modulate the density of pigment in response to ambient light intensity and thereby regulate the amount of light transmitted to the outer segment.[19]

Accumulation of the lipofuscin is one of the most characteristic features of aging observed in retinal pigment epithelial (RPE) cells. The lipofuscin found in RPE cells differs from that of other body tissues because it is derived from the chemically modified residues of incompletely digested photoreceptor outer segments and a mixture of lipids, proteins, and different fluorescent compounds, a derivative of vitamin A.[20] Impairment of normal RPE functions is known to result in retinal degeneration and loss of visual function. It has been reported that a mutation within a gene encoding photoreceptor-specific protein results in massive RPE lipofuscin accumulation and early onset macular degeneration.[21]

At the same time, while reptile and avian species differ in documented maximum life spans, we have little information about whether this is due to the process of senescence, that is, the breakdown of physiological, biochemical, morphological, and/or performance characteristics with age. Taking into consideration that the avian (*Falco tinnunculus tinnunculus* Linnaeus, 1758) and reptilian (*U. aegyptia* (FORSKAL, 1775) are diurnally active, visually oriented animals that are known to possess an excellent, high-acuity visual system and are diurnal species accommodated living in a hard environment of bright and ambient light intensity, they represent good models for illustrating the capability of regenerating photoreceptors as well as the changes of retinal cytostructural elements during the aging process, especially their housing of characteristic features of photoreceptor oil droplet and melanosomes within the pigmented epithelium.

RESULTS AND DISCUSSION

Little is known about the aging-related changes in the ocular region of wild lizard and bird. As we know, the retina represents an integral part of vision by their architecture structure of specialized light-sensitive neuronal cells. The innermost ganglion cells receive the input from the bipolar cells and marking the end of intraretinal processing and the beginning of transmission of the integrated output into the visual cortex.[22] The inner nuclear layers are composed mainly of horizontal and bipolar cells. Bipolar cells are abundant and receive signals from the photoreceptors directly, or via the mediation of a horizontal cell. Their dendrites extend inward in the inner and outer plexiform layer, besides synapses of specifically ganglion cells.[23]

According to Ayoub and Copenhagen,[24] bipolar cells are initiated by synapses with photoreceptors, through release of glutamate by ON- (glutamate hyperpolarization) and OFF-stimuli centers (glutamate depolarization). Ehinger et al.[25] also identified similar expression of glutamate in bipolar cells of the turtle (*Pseudemys scripta elegans*) retina to preserve its visual information from the outer to the inner retina via ON- and OFF-channel pathways.

From the present findings, the retinal thickness of the studied vertebrate species revealed that *F. tinnunculus* possessed marked increase in its thickness of approximately 132.5, 173.7, and 147.8 μm for young, adult, and old age, respectively. However, *U. aegyptia* retinal thickness was 110.2, 148.3, and 130.8 μm. There was a significant change of the whole retinal thickness between the different ages. *F. tinnunculus* possessed characteristic increase of the inner and outer nuclear layers compared with *U. aegyptia*. The increased thickness of outer nuclear layer reflected the increase of cone 's photoreceptors (Figure 1).

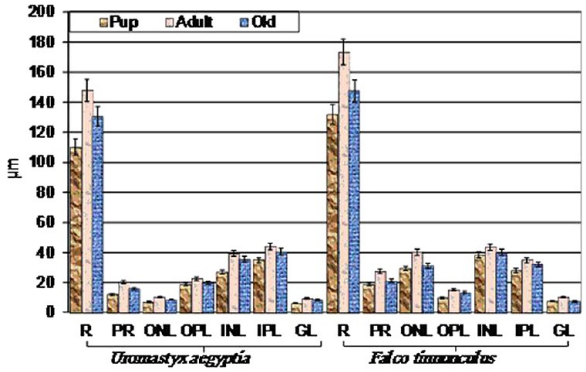

Figure 1. Mean thickness (μm) of retinal cell layer of *U. aegyptia* and *F. tinnunculus*. Data are represented by the mean ± SE. Whole retina thickness is significant at $P < 0.05$.

These seemed to be implicated in the visual acuity allowing *F. tinnunculus* to see prey. Although the inner nuclear cells were less altered with aging, the outer nuclear cells showed apparent damage parallel with deterioration of photoreceptors. Also, old age *U. aegyptia* is more susceptible for aging process compared with *F. tinnunculus*, and this seemed to be attributed to increased Lux light in the lizard habitat compared with that of the bird.

Though light and transmission electron microscopy, the pigmented epithelium showed abundant villous cytoplasmic processes reflecting active phagocytosis and an underlying portion enclosed with abundant melanosomes, mitochondria, and endoplasmic reticulum. The photoreceptor is composed mainly of cones in both species. The distal end of the inner segments showed a prominent oil droplet enclosed almost the aperture of the outer segment (Figures 2−4).

Comparing with pup and adult, in the old age animals, RPE cells exhibited pyknotic nuclei with convolution of the nuclear envelope. There was a marked reduction of melanin granules, vesiculated rough endoplasmic reticulum, degenerated mitochondri,a and presence of numerous lysosomes. The apical pigmented epithelium vesicles in contact with photoreceptors were deteriorated. Old *F. tinnunculus* showed a highest degeneration of oil droplet and accumulation of lipofuscin granules at the apex of the cone outer segment. The gangilion cells showed apparent degeneration. The inner and outer nuclear cells were less affected in Falcon and comparatively damaged in Uromastyx (Figures 2−4). All these manifestations revealed retarded the activity of RPE for phagocytosed the terminal ends of photoreceptors and consequently, reduced its capacity of regeneration.

Melanosomes were found to give higher protection of the retina from sudden bright light by communication through a system of tight junctions directly within the iris muscle that led to harming the retina.[26] Autophagy is a highly conserved intracellular degradative pathway that maintains cellular homeostasis. Mitochondria[27,28] and lysosomes[29] played the important role in the phagocytosis of the RPE.

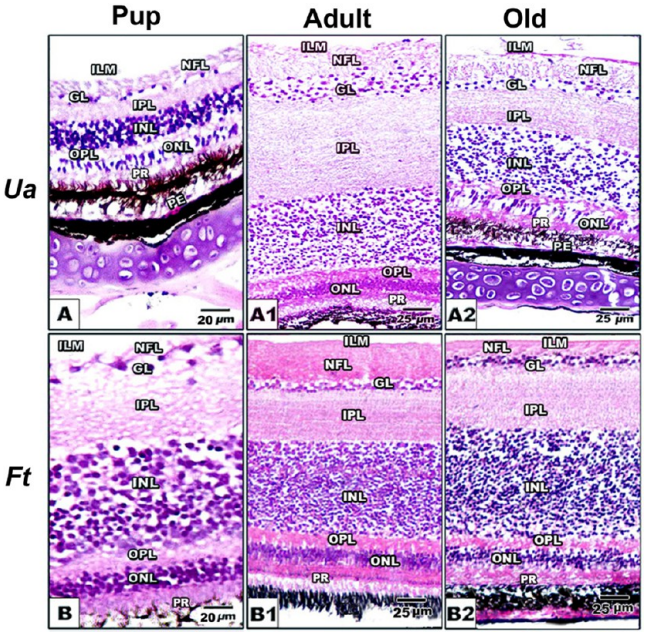

Figure 2. Photomicrographs of transverse histological section of retina of *U. aegyptia* (A–A2) and *F. tinnunculus* (B–B2). (A) Pup *U. aegyptia*, (A1) adult, (A2) old; (B) pup *F. tinnunculus*, (B1) adult, (B2) old. Note that reduction of retinal cell densities and loss of ganglion cells are more detected in *U. aegyptia*. H&E stain.

These findings agree to the work of Salvi et al.[30] who observed similar findings in old patients. Loss of fundus and drusen accumulation were the main results of these cytological alterations.[31,32] Dense accumulation of residual lysosomal bodies containing lipofuscin has been reported in old patients[33] and experimental hamsters,[34] rats,[35] 3 year old Japanese quail,[36] and ABCA4 mouse model.[37]

From our findings, the oil droplet is detected as a characteristic feature at the distal end of the cone inner segment and completely covers the entrance aperture of the outer segment of the pup and adult studied animals (Figures 3 and 4). Similar structural patterns were identified in birds, turtles, lizards, some lungfish,[19] and jungle crow (*Corvus macrorhynchos*).[38] Ohtsuka[39] identified six patterns of cones with color changes of the oil droplets in turtle *Pseudemys scripta elegans* which helps with color discrimination.[40] The oil droplet is heavily pigmented and filters the spectrum of light incident upon the visual pigment within the outer segment.[18,19]

Also, old *U. aegyptia* and *F. tinnunculus* showed deterioration of the oil droplet which led to dramatic effects of light entrance into the retina and enhanced damage of neuronal cells associated with accumulation of lamellated lipofuscin in the apex of the cone outer segment, losing its function and increasing degenerative processes.

Similar findings of photoreceptor cell loss were reported in senile pigeon,[41] reaching approximately 33% of photoreceptors and 23% of gangilion cells. Gradual loss of photoreceptors[42,43] led to impairment of visual function.[44]

Also in old age animals, we detected apparent loss of retinal ganglion cells, especially more in *U. aegyptia* than in *F. tinnunculus*. There was a correlation between the detected demyelination and vacuolation of the nerve axons of the optic nerve and the ganglion cell loss (Figures 4 and 5). The present results supported the work of Harwerth et al.[45] in patients and experimental animals such as rat glaucoma model,[46] burrowing snake's typhlops and Calabaria,[47] and microchiropteran species.[48]

The assessed retinal neurotransmitters reflect the functional activities of retinal neurons. Glycine,[49,50] dopamine (DA),[51] serotonin [52] and glutamate [53] expressed in bipolar cells meanwhile taurine, glutamine, glutamate influenced on gangilion cells[54,55] and horizontal cells.[56] Also, cone photoreceptors play an important role during the transmittion of signals at high temporal frequencies and mediate fine spatial vision. High-frequency transmission requires a high rate of glutamate,[57] glycine [58] release. Glutamate spread from the cone terminal is thought to be limited by presynaptic transporters and nearby glial processes. Dopamine release in response to light and circadian clocks drives daily rhythms of protein phosphorylation in photoreceptor cells.[59] Serotonin was found to induce cone photoreceptor contraction by stimulating dopamine release and consequently, induced light-adaptive retino-motor movements.[60] Modulation of photoreceptor 's function was carried out by. histidine.[61]

From the present findings, we detected that normal retinal neurotransmitter function in pup and adult is higher for *F. tinnunculus* comparing with *U. aegyptia*. This was expressed as a result of increased retinal thickness, mainly the nuclear and photoreceptors layer. However, in old age animals, depletion of the neurotransmitter's amino acids (glutamic, glycine, taurine, glutamine, γ-amino butyric acid, and histidine), serotonin, and dopamines were noticed and seemed to reflect the deterioration of retinal neurons, especially gangilion and nuclear and photoreceptors (Table 1). Similar loss of the neurotransmitters, taurine and glutamate, were reported in dogs with primary glaucoma.[62]

Concerning the optic nerve, we observed demyelination and vacuolation of axons with swelling of mitochondria and vesiculation of the rough and smooth endoplasmic reticulum in their axoplasm (Figure 5). Our findings agree with the findings of Luo et al.[63] in old cat and Mizrahi et al.[64] in elder patients.

Axonal damage of old avian and reptilian species may be attributed to the reduction of retinal gangilion cells,[65] astrocyte hypertrophy,[63] and decreased sufficient oxygen supply.[64] Retinal gangilion cell death was also reported in postexperimental ectomy of optic nerve of rat[66] as a result of cytoplasmic vacuolar degeneration.[67]

The age-related oxidative stresses in the ocular region of the studied animals are very rare. Consider that the eye is an organ that captures light stimuli of the environment and transforms these light signals into nerve impulses that travel through the optic nerve to be processed into images by the brain. The RPE comprises a single layer of polarized cells that separate the photoreceptors from their principal blood supply in the choroid. Oxygen pressure is higher in choroidal blood than in normal peripheral tissues (~60 vs ~40 mmHg, respectively) and contains 1–30 μM H_2O_2.[68,69] Moreover, oxygen consumption is higher in the retina than in most other tissues and 4–5 times higher in old retina than in young retina, yet several enzymes providing protection to oxidative stress are more active in the RPE than in the retina.[70,71]

The assayed CAT, GST, and SOD play an important role in retinal function. Catalase was found to attenuate the injury-induced damage of retinal ganglion and inner plexiform layer and retinal function by enhancing the antioxidative ability and reducing oxidative stresss.[72] Frank et al.[73] detected catalase and superoxide dismutase within RPE of patients.

dx.doi.org/10.1021/cn400154k | ACS Chem. Neurosci. 2014, 5, 39–50

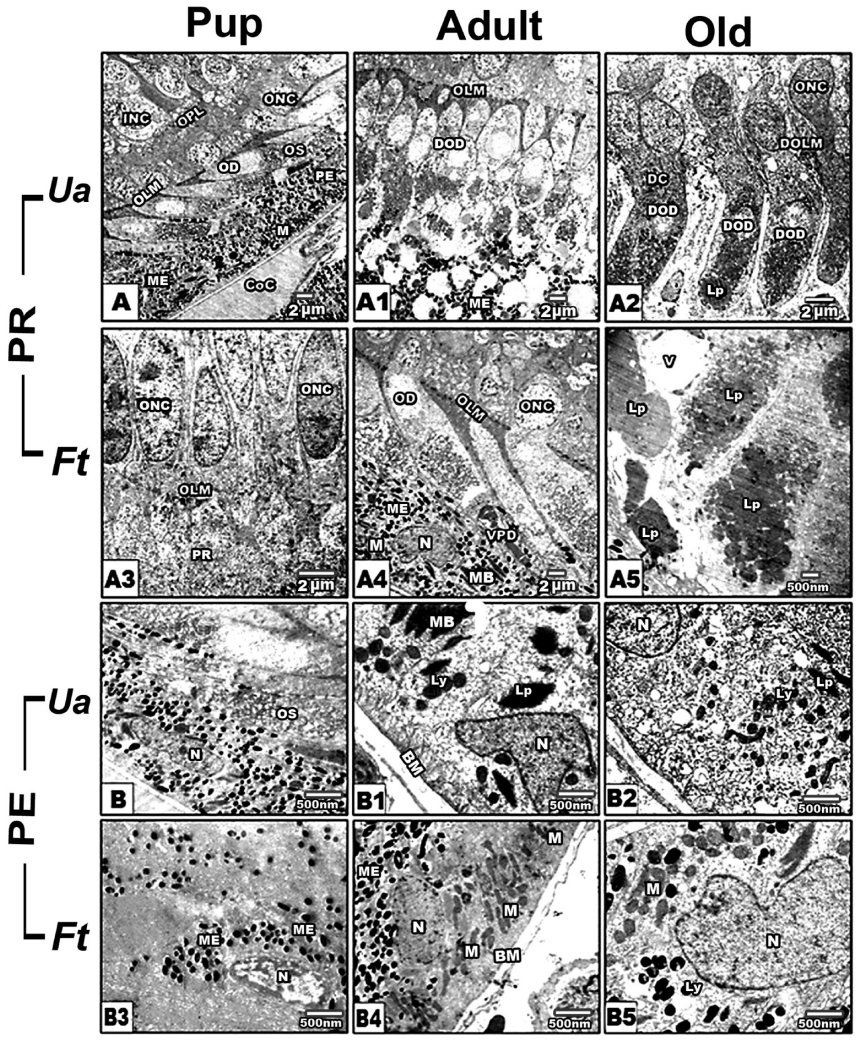

Figure 3. Transmission electron micrographs of retina of *U. aegyptia* (A–A2, B–B2) and *F. tinnunculus* (A3–A5, B3–B5). (A) Pup *U. aegyptius* showing cones containing oil droplet and pigmented epithelium with high dense melanosomes. (A1) Adult showing densely grouping of melanosomes near apical tips of photoreceptors. (A2) Old-age showing apical grouping of lamellated lipofuscin granules and partial missing of oil droplet. (A3) Pup *F. tinnunculus*. (A4) Adult *F. tinnunculus* showing normal photoreceptor outer segment. (A5) Old-age of *F. tinnunculus* showing accumulation of lipofuscins at apexes of photoreceptor outer segment. (B, B3) Pigmented epithelium of pup of *U. aegyptia* and *F. tinnunculus* showing dense grouping of melanosomes. (B1, B4) Adult showing reduction of melanosomes and increase of lysosomes. (B2, B5) Old-age *U. aegyptia* and *F. tinnunculus* showing abundant lysosomes and reduction of melanosomes. Lead citrate and uranyl acetate stains.

Superoxide dismutase catalyzes the dismutation of $O2^-$ into H_2O_2 and O_2. This enzyme has three isoforms, which have been identified in the cornea (epithelium and endothelium),[74] lens epithelium [Ozmen et al., 2002], iris, ciliary body,[75] and retina (inner segment layer of photoreceptor cells and pigment epithelium).[76]

Glutathione S-transferase (GST) is shown to be a dominant, highly expressed enzyme in bovine and mouse RPE microsomes that display significant reduction activity toward synthetic peroxides, oxidized RPE lipids, and oxidized retinoids. The abundance of microsomal glutathione transferase in the RPE underscores its potential importance in oxidative processes in these cells. The major role of the RPE is the phagocytosis and degradation of oxidatively spent rod and cone photoreceptor outer segments, which are unusually rich in docosahexaenoic acid containing lipids, polyunsaturated fatty acids, and retinoids.[77]

We observed activation of the antioxidant enzymes CAT, GST, and SOD during adult age in both retina and optic nerve, then markedly declined in old-age of both species. The decline of the retinal antioxidant activity during the old ages reflects the apparent retinal cell 's deterioration including gangilion, nuclear, cone photoreceptors and RPE. Demyelination of the optic nerve axons and mitochondria within their axoplasm were also detected (Table 2). The observed aging-related depletion of retinal antioxidative stress and retinal damage was confirmed by MDA, the marker of lipid peroxidation and cell damage.[78] The observed findings agree with the work of Hashizume et al.[79] and Yuki et al.[80] in SOD1-deficient mice.

The mitochondria represent the main site of oxygen metabolism accounting for approximately 85–90% of the oxygen consumed by the cell.[2,4] Reactive oxygen species are formed within the mitochondrial matrix.[81] Their biogenesis occurs within the cellular somata of retinal gangilion cells, and then they are transported down the unmyelinated and myelinated axons[83] and regulate the neuronal function. Depletion of the antioxidants and mitochondrial damage may be enhanced by the liberation of superoxide ($O_2^{\bullet-}$) generated

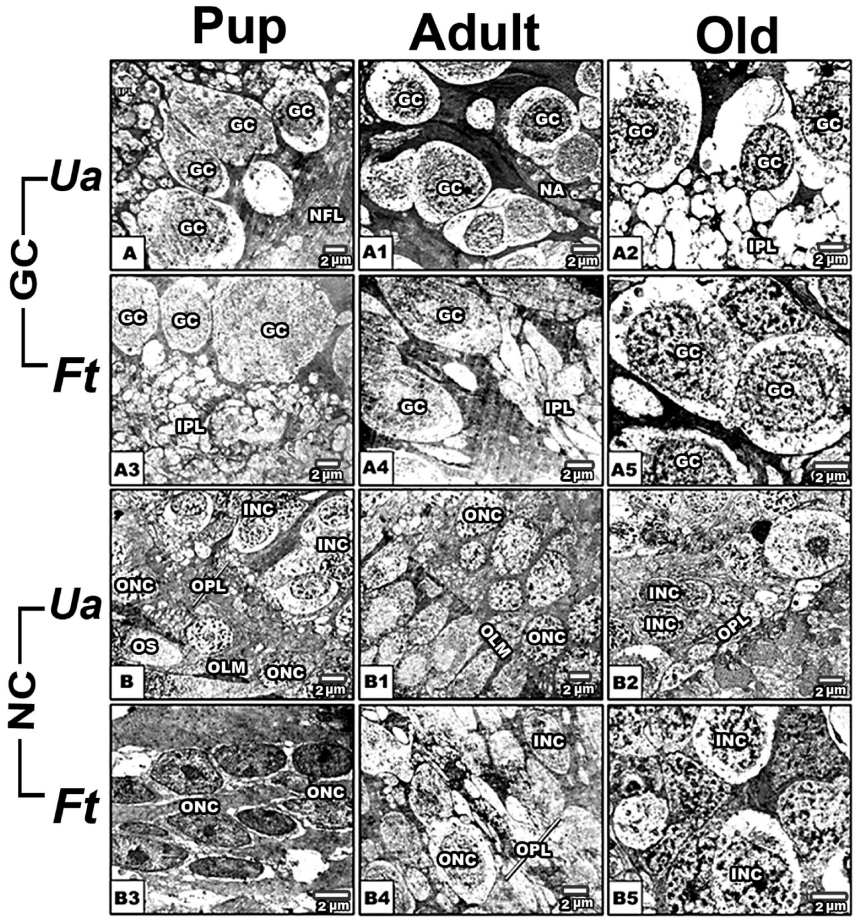

Figure 4. Transmission electron micrographs of retina of *U. aegyptia* (A–A2, B–B2) and *F. tinnunculus* (A3–A5, B3–B5). (A) Pup *U. aegyptia*. (A2) Adult. (A3) Old-age. Note *U. aegyptia* showed normal gangilion cells in pup, which began to vacuolate in shrinkage and degenerated in old age. (A3) Pup *F. tinnunculus*. (A4) Adult. (A5) Old age. Note *F. tinnunculus* shows vacuolation of gangilion cell in old-age. (B) Pup *U. aegyptia*. (B1) Adult. (B2) Old-age. (B3) Pup *F. tinnunculus*. (B4) Adult. (B5) Old age. Note that there are more damaged nuclear cells for *U. aegyptia* than in *F. tinnunculus*. Lead citrate and uranyl acetate stains.

within mitochondria,[84] causing progressive retinal and axonal damage.

Following biochemical analysis of retinal caspase-3 and -7 as well as flow cytometry of DNA cell cycle and P53 of the studied reptilian and avian individuals, we observed increased levels of caspases, increase of M1 (sub-G1 apoptsis), apoptosis, and P53 which coincided with depletion of antioxidive stress and retinal deterioration (Tables 2–4, Figures 6 and 7).

It is well documented that caspases (cysteine aspartate-specific proteases) are the central executioners of apoptosis in a wide range of cell types,[85] especially photoreceptors.[86,87]

Also, P53 was found to knock down in a significant decrease in catalase and Mn-SOD in the retina, more specifically in the retinal gangilion,[88] facilitate lipofuscin accumulation,[89] and activate in response to various cell stress signals, including DNA damage, apoptosis, senescence, and cell cycle arrest.[90]

From our findings, although *U. aegyptia aegyptia* is diurnal, it is a cold-blooded animal basking at the burrow entrance to warm up in the hard desert before heading out to the vegetation with daylight intensity of 10 000–25 000 lx.[91,92] The individuals become inactive during autumn and hibernate in winter. However, *F. tinnunculus tinnunculus* Linnaeus, 1758 is a warm-blooded animal active during the year and builds nests in high latitudes with apparent reduction of light intensity compared with *U. aegyptia*.

Aves have advanced accommodation of vision with light, especially *F. tinnunculus*, which are predatory similar to budgerigar (shell parakeet), *Melopsittacus undulatus* (Psittaciformes), and the zebra finch, *Taeniopygia guttata* (Passeriformes), by the presence of four spectrally distinct classes of the single cone that contains visual pigments absorbing maximally at about 565, 507, 430–445, and 360–380 nm. The three longer-wave cone classes contain colored oil droplets acting as long pass filters with cutoffs at about 570, 500–520, and 445 nm, respectively, whereas the ultraviolet-sensitive cones contain a transparent droplet.[92]

As we mentioned, the studied lizard is subjected to intense sunlight exposure compared with the falcon. The cumulative effects of sunlight exposure and old age increase the oxidative stress and reproduce the retinal and optic damage being recognized in the lizard species.

Exposure of the retina to sunlight led to an increase in the concentrations of polyunsaturated fatty acids and the generation of oxygen species (such as hydrogen peroxide, superoxide anion, hydroxyl radicals, and singlet oxygen) which have an important role in RPE apoptosis and in the development of ocular degeneration.[93]

Exposure at 5000 lx induced hyperactivation of calpains (proteolytic enzymes),[94] suggesting that light-induced retinal damage was caspase-independent and calpain-dependent. In

dx.doi.org/10.1021/cn400154k | *ACS Chem. Neurosci.* 2014, 5, 39–50

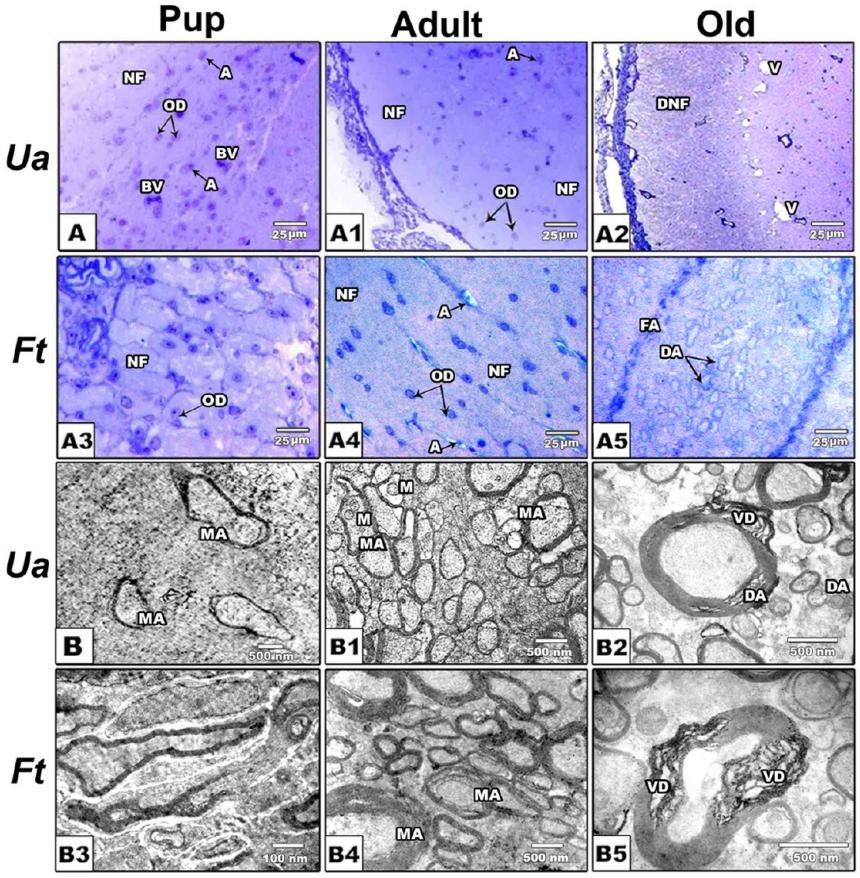

Figure 5. Photomicrographs of toluidine blue stained histological sections (A–A5) and transmission electron micrograghraphs (B–B5) of optic nerve of *U. aegyptia* (A–A2) and *F. tinnunculus* (B–B2). (A, A3) Pup, (A1, A4) adult, (A2, A5) old. Note abundant vacuoles and massive reduction of oligodendrocyte in old age animals. (B–B5) Electron micrographs of optic nerve. (B, B3) Pup, (B1, B4) adult, (B2, B5) old showing demyelination and vacuolation of nerve axon in both species.

albino Sprague–Dawley rats, caspase-3 was overexpressed and activated 8 h after blue light exposure at approximately 60 lx.[87]

Higher intensity of light exposure of the *Uromastyx aegyptia aegyptia* in their habitat reached 10 000–25 000 lx[91,92] in active days with more decreased intensity. The individuals become inactive during autumn and hibernate in winter. However, for *F. tinnunculus tinnunculus* Linnaeus, 1758, this made it highly susceptible to ocular damage.

Finally, the authors concluded that aging altered rentinal and optic nerve structure and function of both species, but more affected in the reptilian species, coincides with a depletion of the neurotransmitters and antioxidant enzymes, parallel to an increase of apoptosis and disruption cell cycles.

METHODS

All experiments were conducted in accordance with the national laws for the use of animals in research and approved by the local ethical committee.

Experimental Work. A selected 90 animals of pup, mid, and old age from *Uromastyx aegyptia aegyptia* (FORSKAL, 1775) (Agamid lizard reptilian species) and *Falco tinnunculus tinnunculus* Linnaeus, 1758) (avian species) (n = 15 per each age) were collected from Sinai and Abou-Rawash district, Giza Governorate, Egypt. Both species are diurnal. *U. aegyptia aegyptia* is cold-blooded animal basking at the burrow entrance to warm up in the hard desert before heading out to forage for leaves, buds, fruits, seeds. and flowers with approximately 12 h of light on and 12 h of light off and daylight intensity 10 000–25 000 lx.[91,92] The individuals become inactive during autumn and hibernate during winter. However, *Falco tinnunculus tinnunculus* Linnaeus, 1758 is a warm-blooded animal active during the year and builds nests in high latitude with apparent reduction of light intensity compared with *U. aegyptia*.

The age was approximately determined according to Bortolotti et al.[96] and using tools available with Adobe Photoshop software. The entire selected area of the iris of American kestrels (*F. tinnunculus*) (i.e., no pupil) was examined. Red, green, and blue values were obtained for different ages of American kestrels.[97] The variations of the color of the iris during aging showed Prout's brown (color 121A) in old age compared with Vandyke brown (color 121) in early life. The irises of the older birds always had a reddish cast to what otherwise appears to be brown. The intermediate age group of 1.5 years appeared to be intermediate in color.

Also, according to Clark,[98] molting of flight feathers can be an aid in determining the age of immatures of species that take more than 1 year of molt to attain adult plumage. Juveniles show no molt. The tail feather pattern varies with each age and can be used for aging. From investigation of the captured specimens, their plumage is mainly light chestnut brown with blackish spots on the upperside and buff with narrow blackish streaks on the underside. According to Casagrande et al.,[99] deep orange-yellow coloration was localized around the nostril, bill, and limbs compared with pale yellowish-white color in juvenile and old age animals. Dense yellow coloration was also detected in the eye lid encircling the eye. The ventral feather of the wing showed intense brown coloration. Also, the wing length was used as an index of age. As an index of body condition, the residuals from the regression of body mass on the cubed wing length were used.[100,101] Hatching dates were determined by visits the nests in the perihatching period.

At the same time, *U. aegyptia* is a herbivorous species captured from the deserts of the east of the Nile river in Egypt. Lizards were kept in an enclosure in a controlled temperature room at 30 °C, with a 12:12

Table 1. Neurotransmitter Levels (μmol/g protein) and Monoaminergic Compounds (ng/mg protein) in Retinas of *U. aegyptia* and *F. timnunculus*[a]

		amino acids (μm/mg)						monoamines (ng/g)		
		Glu	Gly	Tau	His	GABA	Gln	NE	DA	5-HT
Ua	pup	5.32 ± 082	1.90 ± 0.49	3.09 ± 0.11	0.21 ± 0.08	0.91 ± 0.09	1.74 ± 0.27	0.23 ± 0.12	1.87 ± 0.30	0.12 ± 0.05
	adult	4.11 ± 1.37[b]	2.77 ± 0.50[b]	4.12 ± 0.29[b]	0.39 ± 0.11[b]	1.17 ± 0.21[c]	2.25 ± 0.12[c]	0.71 ± 0.33[b]	4.71 ± 1.17[b]	0.15 ± 0.07[b]
	old age	4.57 ± 1.19[b]	1.52 ± 0.21[b]	1.97 ± 0.33[b]	0.25 ± 0.13[b]	1.56 ± 0.31[c]	2.19 ± 0.19[c]	0.54 ± 0.20[b]	3.62 ± 0.33[b]	0.17 ± 0.04[b]
Ft	pup	10.23 ± 1.23	5.52 ± 1.17	8.86 ± 1.44	0.39 ± 0.24	2.01 ± 0.15	2.99 ± 0.27	0.98 ± 0.18	3.12 ± 0.24	0.31 ± 0.09
	adult	12.79 ± 1.78[c]	6.31 ± 1.50[c]	9.27 ± 1.11[b]	0.45 ± 0.17[c]	2.59 ± 0.25[b]	5.02 ± 0.81[b]	1.59 ± 0.14[c]	5.02 ± 1.19[b]	0.39 ± 0.13[c]
	old age	8.56 ± 1.47[c]	8.44 ± 1.33[b]	7.41 ± 1.15[b]	0.75 ± 0.35[b]	1.32 ± 0.09[b]	3.70 ± 0.40[b]	0.76 ± 0.24[b]	4.78 ± 1.31[b]	0.44 ± 0.12[c]

[a]Data are represented as mean ± SE (n = 5). [b]Significant at $P < 0.05$. [c]Nonsignificant at $P < 0.05$.

light cycle. There is no available work dealing with determination of age. From our previous work[102] and Wilm et al.,[103] age determination of the specimens was conducted according to the snout−vent length, length of tail, head width between the anterior margins of the ear openings, head length from the tip of the snout to the anterior margin of the ear opening on the left side, and width of the base tail region.

Morphometry of Retinal Thickness. Retinal thickness was carried out in three selected areas in between the margins of the fovea and cornea of five individuals using a linear occulometer.

Light Microscopic Investigations. Retinas and optic nerves of *U. aegyptia* (1, 24, and 48 months old) and *F. tinnunculus* (1, 12, and 36 months old) were incised immediately, fixed in 10% phosphate-buffered formalin (pH 7.4), dehydrated in ascending grades of ethyl alcohol, cleared in xylol, and mounted in molten pararplast 58−62 °C. Serial 5 μm thick sections were cut and stained with hematoxylin and eosin (H&E), examined under bright field light microscopy, and photographed.

Transmission Electron Microscopy. Extra retina and optic nerve specimens were separated and immediately fixed in 2% glutaraldhyde and 2% paraformaldhyde in 0.1 M cacodylate buffer (pH 7.4). After rinsing in 0.1 M cacodylate buffer, the specimens were postfixed in a buffered solution of 1% osmium tetraoxide at 4 °C for 1.5 h, dehydrated in ascending grades of ethyl alcohol, and embedded in epoxy resin. Ultrathin sections were cut with a LKB Ultratome IV (LKB Instruments, Bromma, Sweden) and mounted on grids, stained with uranyl acetate and lead citrate, and examined on a Joel 100CXl transmission electron microscope (Musashino 3-chome; Akishima, Tokyo, Japan).

Flow Cytometric Analysis of Cell Cycle Apoptosis and P53. DNA ploidy and apoptosis were analyzed using fluorescence activated cell sorting (FACS) flow cytometer (Becton Dickinson, Sunnyvale, CA) equipped with a 15 mW air-cooled 488 nm argon-ion laser. FL1 (FITC) signals were detected through a 530/30 nm band-pass filter; FL2 (PI) signals were detected through a 585/42 nm band-pass filter. A total of 20 000 events were recorded in list mode and analyzed using the Cell Quest Pro software (Becton Dickinson) at Mansoura University Hospital. The cell populations were gated assuming the linear forward scatter (FSC) and side scatter (SSC) properties. Biopsies from retinas and optic nerves of studied animals at the selected ages were taken, and cell suspension was prepared with Tris-EDTA buffer (pH 74) (Sigma-Aldrich Co.). Cell suspension was fixed in ice-cold 96−100% ethanol (Sigma) at 4 °C overnight, centrifuged at 1500 rpm for 10 min, and then resuspended in PBS containing 50 μg/mL propidium iodide (PI) (Sigma-Aldrich Co.). The cells were incubated at 37 °C for 30 min before analysis by flow cytometry. PI fluorescence excitation at 512 nm, with a relatively large Stokes shift, emits at a maximum wavelength of 617 nm. Apoptosis was indicated by the percentage of cells in G0/G1, S, and G2/M phases of the cell cycle.

For P53 labeling, measurements in the fluorescence detector (FL) forward scatter (FSC) and side scatter (SSC) were collected using linear scales. The fluorescence signals were collected using logarithmic scales. Data acquisition and analysis by Cell Quest program (the magnitude of the signal was measured by using cell TM DNA experiment document user's guide 02-61539-00) were performed on 10^4 viable cells. Expression was evaluated as cell percent (the number of stained cells minus the number of cells stained by irrelevant negative control).

Determination of Retinal Neurotransmitters. Retinas and optic nerves were removed quickly from the animal groups, rinsed in cold Tris buffer, and immediately homogenized in 10% ice-cold 2.5 mM-Tris buffer adjusted to pH 7.5 with 1 M HCL, containing 1.0 mM EDTA and centrifuged at 14 000 rpm for 60 min for 5 min at 4 °C. The supernatant was separated and stored in a refrigerator. Following a fluorometric procedure, the acetylcholine (Ach) level was determined according to Gilberstadt and Russell[104] using the following equation: acetylcholine (μM) = optical density of sample − optical density of blank/slope (μM) × n, where n is a dilution factor. Catecholamines, adrenalin and noradrenaline (AD and NAD), 5-HT, and DA were determined fluorometrically as described by Schlumpf et

Table 2. Antioxidants, Malonadialdyde, and Caspase-3 and -7 Levels of Retinal Cells of *U. aegyptia* and *F. tinnunculus*[a]

		CAT (nmol/min/100 mg)	GST (nmol/min/100 mg)	SOD (μ/100 mg)	MD (μmol/100 mg)	CAS-3 (μ/100 mg)	CAS-7 (ng/100 mg)
retina							
Ua	pup	5.25 ± 1.51	4.20 ± 0.81	50.37 ± 1.49	6.10 ± 1.74	0.178 ± 0.01	3.812 ± 0.15
	adult	5.66 ± 0.97[c]	6.66 ± 1.11[b]	57.14 ± 2.13[b]	7.35 ± 1.20[c]	0.37 ± 0.02[b]	4.64 ± 0.13[b]
	old age	4.55 ± 1.97[c]	3.78 ± 0.49[b]	43.3 ± 1.59[b]	11.27 ± 2.41[c]	0.46 ± 0.01[b]	6.01 ± 0.12[b]
Ft	pup	5.67 ± 0.26	4.50 ± 0.42	74.69 ± 2.37	10.32 ± 0.74	0.23 ± 0.02	2.38 ± 0.21
	adult	8.66 ± 1.40[c]	5.82 ± 0.48[b]	84.93 ± 2.43[b]	12.95 ± 1.24[b]	0.32 ± 0.03[b]	3.85 ± 0.24[b]
	old age	7.65 ± 0.68[c]	3.03 ± 0.51[b]	58.15 ± 1.21[b]	18.15 ± 0.85[b]	0.47 ± 0.07[b]	5.56 ± 0.49[b]
optic nerve							
Ua	pup	9.63 ± 0.74	3.02 ± 0.48	48.60 ± 2.13	7.36 ± 1.21	0.19 ± 0.02	2.87 ± 0.21
	adult	11.51 ± 0.36[c]	4.66 ± 0.63[b]	52.46 ± 2.11[b]	13.72 ± 1.62[c]	0.39 ± 0.03[b]	4.54 ± 0.18[b]
	old age	7.90 ± 0.17[c]	3.88 ± 0.46[b]	44.42 ± 2.98[b]	18.71 ± 1.99[c]	0.45 ± 0.03[b]	4.93 ± 0.27[b]
Ft	pup	7.21 ± 0.24	3.24 ± 0.27	82.91 ± 2.43[b]	13.47 ± 0.90	0.35 ± 0.02	4.22 ± 0.87
	adult	10.80 ± 0.70[c]	5.24 ± 0.16[b]	74.77 ± 2.58[b]	19.32 ± 1.22[c]	0.39 ± 0.09[b]	5.04 ± 0.42[b]
	old age	8.22 ± 0.29[c]	2.22 ± 0.13[b]	60.23 ± 2.62[b]	22.73 ± 1.02[c]	0.53 ± 0.04[b]	7.54 ± 0.63[b]

[a]Data are represented as mean ± SE (n = 5). [b]Nonsignificant at $P < 0.05$. [c]Significant at $P < 0.05$.

Table 3. Flow Cytometry of Percentages of Apoptosis and P53 of Retina during Aging of *U. aegyptia* and *F. tinnunculus*[a]

		U. aegyptia			*F. tinnunculus*		
		pup	adult	old	pup	adult	old
cell cycle	M1 (sub-G0/G1 apoptosis)	12.63 ± 2.87	28.70 ± 3.23[b]	50.49 ± 4.89[b]	32.99 ± 3.7	53.95 ± 3.03[b]	70.36 ± 4.24[b]
	M2 (G0/1 phase)	8.58 ± 1.98	7.61 ± 2.57[b]	29.42 ± 4.74[b]	9.45 ± 2.65	15.45 ± 3.4[b]	21.59 ± 1.98[b]
	M3 (S phase)	3.41 ± 1.19	3.48 ± 0.66[c]	9.18 ± 2.38[b]	3.55 ± 1.48	6.06 ± 1.81[c]	4.79 ± 1.42[c]
	M4 (G2/M phase)	0.87 ± 0.11	0.57 ± 0.12[c]	3.06 ± 1.43[c]	1.02 ± 0.22	0.56 ± 0.18[c]	2.30 ± 1.03[c]
P53		32.57 ± 3.45	25.03 ± 4.77[c]	46.15 ± 4.12[b]	23.45 ± 2.88	54.76 ± 3.73[c]	70.27 ± 4.12[b]

[a]Data are represented by the mean ± SE (n = 5). M1−M4 phases of cell cycles represented as percentages of total 100%. [b]Significant at $P < 0.05$. [c]Nonsignificant at $P < 0.05$.

Table 4. Flow Cytometry of Percentages of Apoptosis and P53 of Optic Nerve during Aging of *U. aegyptia* and *F. tinnunculus*[a]

		U. aegyptia			*F. tinnunculus*		
		pup	adult	old	pup	adult	old
cell cycle	M1 (sub-G0/G1 apoptosis)	22.83 ± 2.67	56.44 ± 3.88[b]	70.33 ± 4.32[b]	22.14 ± 2.87	42.21 ± 4.45[b]	66.06 ± 5.09[b]
	M2 (G0/1 phase)	54.00 ± 4.98	25.10 ± 2.51[b]	11.96 ± 1.38[b]	56.71 ± 6.49	19.75 ± 1.7[b]	18.81 ± 1.63[b]
	M3 (S phase)	15.70 ± 3.01	7.11 ± 2.86[b]	7.23 ± 1.28[b]	14.72 ± 2.39	9.88 ± 1.22[b]	6.36 ± 1.57[b]
	M4 (G2/M phase)	8.97 ± 1.73	2.07 ± 0.83[b]	0.74 ± 0.39[b]	7.82 ± 0.89	3.92 ± 0.78[b]	2.35 ± 0.61[b]
P_{53}		14.72 ± 2.17	23.34 ± 2.90[b]	45.98 ± 3.08[b]	14.40 ± 1.99	29.76 ± 2.59[b]	53.43 ± 3.97[b]

[a]Data are represented by the mean ± SE (n = 5). M1−M4 phases of cell cycles represented as percentages of total 100%. [b]Significant at $P < 0.05$.

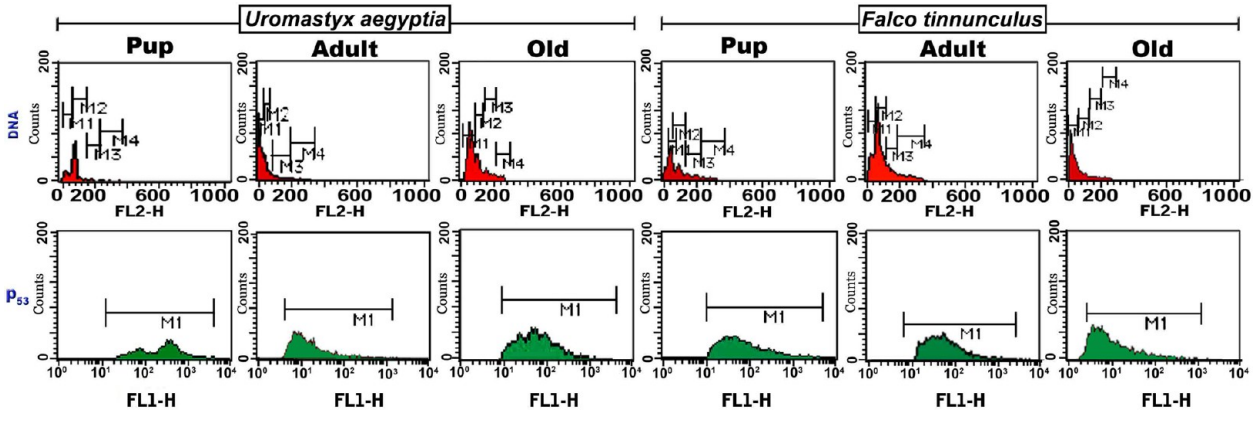

Figure 6. Flow cytometry chart of DNA and P53 of retina of pup, adult, and old *U. aegyptia* and *F. tinnunculus* aged 6, 18, 24, and 30 months. M1 DNA and P53 show marked increase. FL1 detector, fluorescence. FL2 detector, fluorescence of propidium iodide stain phycoerythrin orange (PI).

dx.doi.org/10.1021/cn400154k | ACS Chem. Neurosci. 2014, 5, 39−50

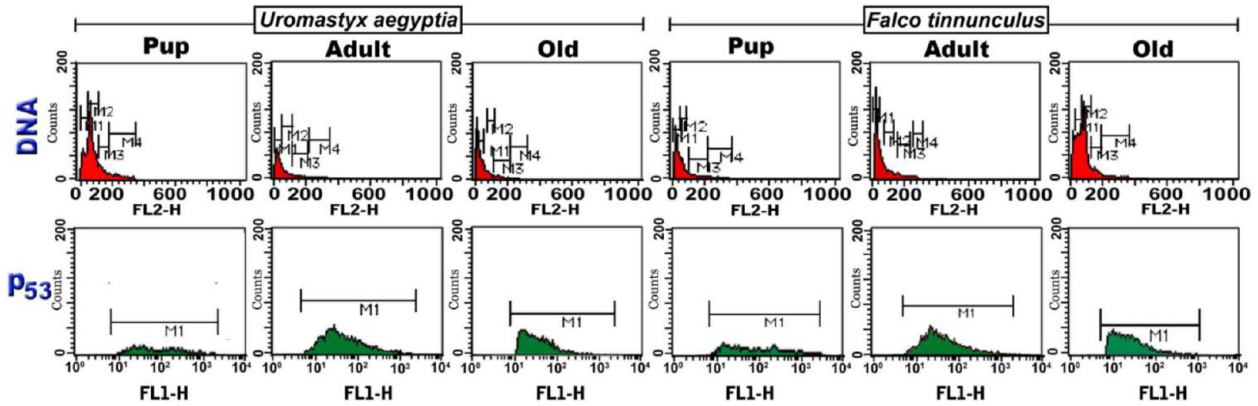

Figure 7. Flow cytometry chart of DNA and P53 of optic nerve of pup, adult, and old *U. aegyptia* and *F. tinnunculus* aged 6, 18, 24, and 30 months. M1 DNA and P53 showing marked increase. FL1 detector, fluorescence. FL2 detector, fluorescence of propidium iodide stain phycoerythrin orange (PI).

al.[105] Retinal free amino acids, glutamic acid, aspartic acid, asparagine, GABA (γ-amino- butyric acid), glycine, taurine, and histidine were determined by high performance liquid chromatography (HPLC) using the precolumn phenylthiocarbamyl (PTC) derivatization technique according to the method of Heinrikson and Meredith.[106]

Biochemical Assessments of Catalase, Glutathione S-Transferase, and Superoxide Dismutase. Known weights of retinas and optic nerves of aged reptilian and aves individuals were homogenated and kept in refrigerator at −20 °C. Catalase is an antioxidant enzyme involved in the detoxification of hydrogen peroxide and was determined according to Bock et al.[107] In brief, the tissue homogenate was further diluted by phosphate buffer (pH 7.0). The reaction mixture (containing 0.05 M phosphate buffer (pH 7.0), 1.2 mM H_2O_2, and 0.2 mL of homogenate) was allowed to stand for 30 min. The absorbance of the sample was read against distilled water at 240 nm.

Glutathione S-transferase (GST) activity was measured according to Habig et al.[108] by measuring the conjugation of 1-chloro-2,4-dinitrobenzene (CDNB) with reduced glutathione, and absorbance was determined at 340 nm.

Superoxide dismutase (SOD) activity was determined according to Niskikimi et al.[109] based on adding 1.8 mL of sodium pyrophosphate buffer, 0.5 mL of working nitroblue tetrazolium, 0.5 mL of reduced nicotinamide-adenine dinucleotide (NADH), and 0.1 mL of tissue homogenate, plus 0.1 mL of freshly prepared working phenazine methosulphate. Reaction was initiated by the addition of phenazine methosulphate and absorbance red at 560 nm.

Determination of Lipid Peroxidation End Product Malondialdehyde (Thiobarbituric Acid Reactive Substances, TBARS) Level. Lipid peroxidation end product malondialdhyde was determined according to Ohkawa et al.[110] Two hundred microliters of tissue homogenate supernatant was added to 100 μL of sodium dodecyl sulfate (SDS), 750 μL of 20% acetic acid (pH 3.5), 750 μL of 0.6% thiobarbituric acid, and 300 μL of distilled water, and the mixture was incubated at 95 °C for 60 min. After addition of 2.5 mL of butanol/pyridine (15:1) and 500 μL of distilled water, the solution was vortexed and then centrifuged at 2000*g* for 15 min. A reddish-pink color developed and was analyzed at 532 nm.

Biochemical Assessments of Caspse-3 and -7. Caspase-3 is an intracellular cysteine protease that exists as a proenzyme, becoming activated during the sequence of events associated with apoptosis. It is determined colorimetrically by using a Stressgen kit (catalog no. 907-013). Retinal cells were lysed to collect their intracellular contents, and the lysate tested for protease activity by the addition of a caspase-specific peptide that is conjugated to the color reporter molecule *p*-nitroaniline (pNA). The cleavage of the peptide can be quantitated spectrophotometrically at a wavelength of 405 nm. The level of caspase enzymatic activity in the cell lysate is directly proportional to the color reaction.

Caspase-7 is a member of the caspase (cysteine aspartate protease) family of proteins and was determined by using an ELISA kit (Uscn Life Science Inc., Wuhan, China, cat. no. E0449Ra). The microtiter plate provided in this kit is precoated with an antibody specific to caspase-7. Standards or samples are then added to the appropriate microtiter plate wells with a biotin-conjugated polyclonal antibody preparation specific for caspase-7. Next, avidin conjugated to horseredish peroxidase (HRP) is added to each microplate well and incubated, and then a TMB substrate solution is added to each well. Only those wells that contain caspase-7, biotin-conjugated antibody, and enzyme-conjugated avidin will exhibit a color change. The enzyme−substrate reaction is terminated by the addition of a sulfuric acid solution, and the color change is measured spectrophotometrically at a wavelength of 450 nm . The concentration of caspase-7 in the samples is determined by comparing the optical density of the samples to a standard curve.

Statistical Analysis. Data are presented as means ± standard error (SE). The statistical analysis was performed with multivariant analysis of variance (MANOVA) using the SPSS (version 16) software package for Windows (SPSS 15.0; SPSS, Chicago, IL), comparing the multivariations between aged-animal groups in the same group, as well as among different classes. The *F*-test was calculated and considered statistically significant at $p < 0.05$.

AUTHOR INFORMATION

Corresponding Author

*E-mail: elsayyad@mans.edu.eg. Telephone: 0020 502254850. Fax: 0020 50 2246781.

Author Contributions

H. I. H. El-Sayyad and A. A. El-Mansy take samples and conducted light and ultrastructure experiments, and carried out the neurotransmitters, antioxidative stress, flow cytometry, and statistical analysis. A. S. AL-Gebaly did comments of histopathological and ultrastructural observations. S. A. Khalifa did the statistical analysis. All the authors participated in the experimental design and writing of the paper.

Notes

The authors declare no competing financial interest.

ABBREVIATIONS

A, astrocyte; BM, basement membrane; BV, blood vessel; CAT, catalase; Cas-3, caspase-3; Cas-7, caspase-7; CoC, choriocapillaries; DA, dopamine; DAs, degenerated axons; DC, double cone; DMA, demyelinated axons; DOLM, degenerated outer limiting membrane; DOD, degenerated oil droplet; FA, fascicles of axon; Ft, *F. tinnunculus*; GL, ganglion layer; Glu, glutamic acid; Gly, glycine; GABA, γ-aminobutyric acid; Gln, glutamine; GST, glutathione-S-transferase; His, histidine; 5-

HT, 5-hydroxytryptamine (serotonin); IPL, inner plexiform layer; INL, inner nuclear layer; ILM, inner limiting membrane; M, mitochondria; MA, myelinated axon; MD, malondialdehyde; N, nucleus; NE, norepinephrine; NFL, nerve fiber layer; ONL, outer nuclear layer; OPL, outer plexiform layer; OD, oil droplet; ODt, oligodendrocyte; OS, outer segment; ON, outer nuclear; OLM, outer limiting membrane; PE, pigmented epithelium; PR, photoreceptor; SOD, superoxide dismutase; Tau, taurine; Ua, *U. aegyptia*; V, vacuoles; VD, vacuolar degeneration; VPD, visual pigmented disc

REFERENCES

(1) Harman, D. (1981) The aging process. *Proc. Natl. Acad. Sci. U.S.A. 78*, 7124−7128.

(2) Schachar, R. A. (2006) Effect of change in central lens thickness and lens shape on age-related decline in accommodation. *J. Cataract Refractive Surg. 32*, 1897−1898.

(3) Smith, W., Assink, J., Klein, R., Mitchell, P., Klaver, C. C., Klein, B. E., Hofman, A., Jensen, S., Wang, J. J., and de Jong, P. T. (2001) Risk factors for age-related macular degeneration: pooled findings from three continents. *Ophthalmology 108*, 697−704.

(4) Jager, R. D., Mieler, W. F., and Miller, J. W. (2008) Age-related macular degeneration. *N. Engl. J. Med. 358*, 2606−2617.

(5) Zhdankina, A., Fursova, A. Z., Logvinov, S. V., and Kolosova, N. G. (2008) Clinical and morphological characteristics of chorioretinal degeneration in early aging OXYS rats. *Bull. Exp. Biol. Med. 146*, 455−458.

(6) Markovets, A. M., Saprunova, V. B., Zhdankina, A. A., Fursova, A. Z., Bakeeva, L. E., and Kolosova, N. G. (2011) Alterations of retinal pigment epithelium cause AMD-like retinal damage in senescence-accelerated OXYS rats. *Aging (N. Y.). 3*, 44−54.

(7) Pow, D. V., and Diaz, C. M. (2008) AMD-like Lesions in the Rat Retina: A Latent Consequence of Perinatal Hemorrhage. *Invest. Ophthalmol. Visual Sci. 49*, 2790−798.

(8) Rocher, N., Behar-Cohen, F., Pournaras, J. A., Naud, M. C., Jeanny, J. C., Jonet, L., and Bourges, J. L. (2011) Effects of rat anti-VEGF antibody in a rat model of corneal graft rejection by topical and subconjunctival routes. *Mol. Vision 17*, 104−112.

(9) Winkler, B. S., Boulton, M. E., Gottsch, J. D., and Sternberg, P. (1999) Oxidative damage and age-related macular degeneration. *Mol. Vision 5*, 32.

(10) Louie, J., Kapphahn, R., and Ferrington, D. (2002) Proteasome function and protein oxidation in the aged retina. *Exp. Eye Res. 75*, 271−284.

(11) Bayón, A., Almela, R. M., and Talavera, J. (2007) Avian ophthalmology. *Eur. J. Companion Anim. Pract. 17*, 1−13.

(12) Young, S. R., and Martin, G. R. (1984) Optics of retinal oil droplets:A model of light collection and polarization detection in the avian retina. *Vision Res. 24*, 129−137.

(13) Bowmaker, J. K., Loew, E. R., and Ott, M. (2005) The cone photoreceptors and visual pigments of chameleons. *J. Comp. Physiol. A . 191*, 925−932.

(14) Jones, O. R., Gaillard, J. M., Tuljapurkar, S., Alho, J. S., Armitage, K. B., Becker, P. H., et al. (2008) Senescence rates are determined by ranking on the fast-slow life-history continuum. *Ecol. Lett. 11*, 664−673.

(15) Bonduriansky, R., and Brassil, C. E. (2005) Reproductive ageing and sexual selection on male body size in a wild population of antler flies (Protopiophila litigata). *Evol. Biol. 18*, 1332−1340.

(16) Congdon, J. D., Nagle, R. D., Kinney, O. M., van Loben Sels, R. C., Quinter, T., and Tinkle, D. W. (2003) Testing hypotheses of aging in long-lived painted turtles (*Chrysemys picta*). *Exp. Gerontol. 38*, 765−772.

(17) Forslund, P., and Part, T. (1995) Age and reproduction in birds − hypotheses and tests. *Trends Ecol. Evol. 10*, 374−378.

(18) Vorobyev, M. (2003) Coloured oil droplets enhance colour discrimination. *Proc. R. Soc. London, Ser. B 270*, 1255−1261.

(19) Hart, N. S., Lisney, T. J., and Collin, S. P. (2006) Cone photoreceptor oil droplet pigmentation is affected by ambient light intensity. *J. Exp. Biol. 209*, 4776−4787.

(20) Kennedy, C. J., Rakoczy, P. E., and Constable, I. J. (1995) Lipofuscin of the retinal pigment epithelium: a review. *Eye (London, U.K.). 9*, 763−771.

(21) Katz, M. L. (2002) Potential role of retinal pigment epithelial lipofuscin accumulation in age-related macular degeneration. *Arch. Gerontol. Geriatr. 34*, 359−370.

(22) Abbas, S. Y., Hamade, K. C., Yang, E. J., Nawy, S., Smith, R. G., and Pettit, D. L. (2013) Directional summation in non-direction selective retinal ganglion cells. *PLoS Comput. Biol. 9*, e1002969.

(23) Werblin, F. S., and Dowling, J. E. (1969) Organization of the retina of the mudpuppy, Necturus maculosus. II.Intracellular recording. *J. Neurophysiol. 32*, 339−355.

(24) Ayoub, G. S., and Copenhagen, D. R. (1991) Application of a fluorometric method to measure glutamate release from single retinal photoreceptors. *J. Neurosci. Methods. 37*, 7−14.

(25) Ehinger, B., Ottersen, O. P., Storm-Mathisen, J., and Dowling, J. E. (1988) Bipolar cells in the turtle retina are strongly immunoreactive for glutamate. *Proc. Natl. Acad. Sci. U.S.A. 85*, 8321−8325.

(26) Moyer, F. H. (1969) Development, structure and function of the retinal pigment epithelium. In *The Retina* (Straatsma, B. R., Hall, M. O., Allen, R. A., and Crescitelli, F., Eds), pp 1−30, University of California Press, Los Angeles.

(27) Braekevelt, C. R. (1994) Retinal pigment epithelial fine structure in the American crow (Corvus brachyrhynchos). *Anat., Histol., Embryol. 23*, 367−375.

(28) Miceli, M. V., Liles, M. R., and Newsome, D. A. (1994) Evaluation of oxidative processes in human pigment epithelial cells associated with retinal outer segment phagocytosis. *Exp. Cell Res. 214*, 242−249.

(29) Zinn, K. M. and Benjamin-Henkind, J. V. (1979) Anatomy of the human retinal pigment epithelium. In *The Retinal Pigment Epithelium* (Zinn, K. M., and Marmor, M. F., Eds.), pp 3−31, Harvard University Press, Cambridge, MA.

(30) Salvi, S. M., Akhtar, S., and Currie, Z. (2006) Ageing changes in the eye. *Postgrad. Med. J. 82*, 581−587.

(31) Rodríguez-Muela, N., Koga, H., García-Ledo, L., de la Villa, P., de la Rosa, E. J., Cuervo, A. M., and Boya, P. (2013) Balance between autophagic pathways preserves retinal homeostasis. *Aging Cell 12*, 478−488.

(32) Sarna, T., Pilas, B., Land, E. J., and Truscott, T. G. (1986) Interaction of radicals from water radiolysis with melanin. *Biochim. Biophys. Acta 883*, 162−167.

(33) Rodríguez-Muela, N., Koga, H., García-Ledo, L., de la Villa, P., de la Rosa, E. J., Cuervo, A. M., and Boya, P. (2013) Balance between autophagic pathways preserves retinal homeostasis. *Aging Cell 12*, 478−488.

(34) Morales, E., Horn, R., Pastor, L. M., Santamaría, L., Pallarés, J., Zuasti, A., Ferrer, C., and Canteras, M. (2004) Involution of seminiferous tubules in aged hamsters: an ultrastructural, immunohistochemical and quantitative morphological study. *Histol. Histopathol. 19*, 445−455.

(35) Kubasik-Juraniec, J., Kmieć, Z., Tukaj, C., Rudzińska-Kisiel, T., Kotlarz, G., Pokrywka, L., and Myśliwski, A. (2004) The effect of fasting and refeeding on the ultrastructure of the hypothalamic paraventricular nucleus in young and old rats. *Folia Morphol. (Warsaw) 63*, 25−35.

(36) Fite, K. V., and Bengston, L. (1989) Aging and sex-related changes in the outer retina of Japanese quail. *Curr. Eye Res. 8*, 1039−1048.

(37) Radu, R. A., Yuan, Q., Hu, J., Peng, J. H., Lloyd, M., Nusinowitz, S., Bok, D., and Travis, G. H. (2008) Accelerated accumulation of lipofuscin pigments in the RPE of a mouse model for ABCA4-mediated retinal dystrophies following Vitamin A supplementation. *Invest. Ophthalmol. Visual Sci. 49*, 3821−3829.

(38) Rahman, M. L., Yoshida, K., Maeda, I., Tanaka, H., and Sugita, S. (2010) Distribution of retinal cone photoreceptor oil droplets, and

identification of associated carotenoids in crow (*Corvus macrorhynchos*). *Zool. Sci. 27*, 514−521.
(39) Ohtsuka, T. (1985) Relation of spectral types to oil droplets in cones of turtle retina. *Science 229*, 874−877.
(40) Knott, B., Berg, M. L., Morgan, E. R., Buchanan, K. L., Bowmaker, J. K., and Bennett, A. D. (2010) Avian retinal oil droplets: dietary manipulation of colour vision? *Proc. Biol. Sci. 277*, 953−962.
(41) Hodos, W., Miller, R. F., and Fite, K. V. (1991) Age-dependent changes in visual acuity and retinal morphology in pigeons. *Vision Res. 31*, 669−677.
(42) Gresh, J., Goletz, P. W., Crouch, R. K., and Rohrer, B. (2003) Structure and function analysis of rods and cones in juvenile, adult, and aged C57bl06 and Balb0c. *Visual Neurosci. 20*, 211−220.
(43) Jackson, G. R., McGwin, G., Phillips, J. M., Klein, R., and Owsley, C. (2006) Impact of aging and age-related maculopathy on inactivation of the a-wave of the rod-mediated electroretinogram. *Vision Res. 46*, 1422−1431.
(44) Spear, P. D. (1993) Neural bases of visual deficits during aging. *Vision Res. 33*, 2589−609.
(45) Harwerth, R. S., Wheat, J. L., and Rangaswamy, N. V. (2008) Age-related losses of retinal ganglion cells and axons. *Invest. Ophthalmol. Visual Sci. 49*, 4437−4443.
(46) Danias, J., Shen, F., Kavalarakis, M., Chen, B., Goldblum, D., Lee, K., Zamora, M. F., Su, Y., Brodie, S. E., Podos, S. M., and Mittag, T. (2006) Characterization of retinal damage in the episcleral vein cauterization rat glaucoma model. *Exp. Eye Res. 82*, 219−228.
(47) Reperant, J., Miceli, D., Rio, J., and Weidner, C. (1987) The primary optic system in a microphthalmic snake (Calabria retinhardti). *Brain Res. 408*, 233−238.
(48) Pettigrew, J., Dreher, B., Hopkins, C., McCall, M., and Brown, M. (1988) Peak density and distribution of ganglion cells in the retinae of microchiropteran bats. Implications for visual acuity. *Brain Behav. Evol. 32*, 39−56.
(49) Jusuf, P. R., Haverkamp, S., and Grünert, U. (2005) Localization of glycine receptor alpha subunits on bipolar and amacrine cells in primate retina. *J. Comp. Neurol. 488*, 113−128.
(50) Zhou, C., and Dacheux, R. F. (2005) Glycine- and GABA-activated inhibitory currents on axon terminals of rabbit cone bipolar cells. *Visual Neurosci. 22*, 759−767.
(51) Newkirk, G. S., Hoon, M., Wong, R. O., and Detwiler, P. B. (2013) Inhibitory inputs tune the light response properties of dopaminergic amacrine cells in mouse retina. *J Neurophysiol. 110*, 536−552.
(52) Ochoa-de la Paz, L. D., Estrada-Mondragón, A., Limón, A., Miledi, R., and Martínez-Torres, A. (2012) Dopamine and serotonin modulate human GABAρ1 receptors expressed in Xenopus laevis oocytes. *ACS Chem. Neurosci. 3*, 96−104.
(53) Wu, S. M. (1994) Synaptic transmission in the outer retina. *Annu. Rev. Physiol. 56*, 141−168.
(54) Fu, C. T., and Sretavan, D. W. (2012) Ectopic vesicular glutamate release at the optic nerve head and axon loss in mouse experimental glaucoma. *Neuroscience 32*, 15859−15876.
(55) Jiang, Z., Bulley, S., Guzzone, J., Ripps, H., and Shen, W. (2013) The modulatory role of taurine in retinal ganglion cells. *Adv. Exp. Med. Biol. 775*, 53−68.
(56) Wu, S. M. (1994) Synaptic transmission in the outer retina. *Annu. Rev. Physiol. 56*, 141−168.
(57) Szmajda, B. A., and Devries, S. H. (2011) Glutamate spillover between mammalian cone photoreceptors. *J. Neurosci. 31*, 13431−3441.
(58) Shen, W., Jiang, Z., and Li, B. (2008) Glycine input induces the synaptic facilitation in salamander rod photoreceptors. *J. Biomed. Sci. 15*, 743−754.
(59) Pozdeyev, N., Tosini, G., Li, L., Ali, F., Rozov, S., Lee, R. H., and Iuvone, P. M. (2008) Dopamine modulates diurnal and circadian rhythms of protein phosphorylation in photoreceptor cells of mouse retina. *Eur. J. Neurosci. 27*, 2691−2700.
(60) Dearry, A., and Burnside, B. (1986) Dopaminergic regulation of cone retinomotor movement in isolated teleost retinas: II. Modulation by gamma-aminobutyric acid and serotonin. *J. Neurochem. 46*, 1022−1031.
(61) Zhu, Y., Mistra, S., Nivison-Smith, L., Acosta, M. L., Fletcher, E. L., and Kalloniatis, M. (2013) Mapping cation entry in photoreceptors and inner retinal neurons during early degeneration in the P23H-3 rat retina-CORRIGENDUM. *Visual Neurosci. 30* (5), 1−11.
(62) Madl, J. E., McIlnay, T. R., Powell, C. C., and Gionfriddo, J. R. (2005) Depletion of taurine and glutamate from damaged photoreceptors in the retinas of dogs with primary glaucoma. *Am. J. Vet. Res. 66*, 791−799.
(63) Luo, X., Hua, T. M., Sun, Q. Y., Mei, B., Zhu, Z. M., and Zhang, C. Z. (2006) Age-related morphological changes in the optic nerve of the cat. *Acta Zool. Sin. 52*, 182−189.
(64) Mizrahi, H., Hugkulstone, C. E., Vyakarnam, P., and Parker, M. C. (2011) Bilateral ischaemic optic neuropathy following laparoscopic proctocolectomy: a case report. *Ann. R. Coll. Surg. Engl. 93*, e53−54.
(65) Bergman, E., and Ulfhake, B. (1998) Loss of primary sensory neurons in the very old rat: neuron number estimates using the disector method and confocal optical sectioning. *J. Comp. Neurol. 396*, 211−222.
(66) Villegas-Pérez, M. P., Vidal-Sanz, M., Rasminsky, M., Bray, G. M., and Aguayo, A. J. (1993) Rapid and protracted phases of retinal ganglion cell loss follow axotomy in the optic nerve of adult rats. *J. Neurobiol. 24*, 23−36.
(67) Germain, F., Fernández, E., and de la, V. P. (2007) Morphological signs of apoptosis in axotomized ganglion cells of the rabbit retina. *Neuroscience 144*, 898−910.
(68) Garcia-Castineiras, S., Velazquez, S., Martinez, P., and Torres, N. (1992) Aqueous humor hydrogen peroxide analysis with dichlorophenol-indophenol. *Exp. Eye Res. 55*, 9−19.
(69) Spector, A., Ma, W., and Wang, R. R. (1998) The aqueous humor is capable of generating and degrading H2O2. *Invest. Ophthalmol. Visual Sci. 39*, 1188−1197.
(70) Cohen, L. H., and Noell, W. K. (1960) Glucose catabolism of rabbit retina before and after development of visual function. *J. Neurochem. 5*, 253−276.
(71) Hess, R., and Pearse, A. G. (1961) Histochemical demonstration of uridine diphosphate glucose dehydrogenase. *Experientia 17*, 317−318.
(72) Chen, B., and Tang, L. (2011) Protective effects of catalase on retinal ischemia/reperfusion injury in rats. *Exp. Eye Res. 93*, 599−606.
(73) Frank, R. N., Amin, R. H., and Puklin, J. E. (1999) Antioxidant enzymes in the macular retinal pigment epithelium of eyes with neovascular age-related macular degeneration. *Am. J. Ophthalmol. 127*, 694−709.
(74) Behndig, A., Karlsson, K., Johansson, B. O., Brannstrom, T., and Marklund, S. L. (2001) Superoxide dismutase isoenzymes in the normal and diseased human cornea. *Invest. Ophthalmol. Visual Sci. 42*, 2293−2296.
(75) Phylactos, A. C., and Unger, W. G. (1998) Biochemical changes induced by intravitreally-injected doxorubicin in the iris-ciliary body and lens of the rabbit eye. *Doc. Ophthalmol. 95*, 145−155.
(76) Agardh, C. D., Gustavsson, C., Hagert, P., Nilsson, M., and Agardh, E. (2006) Expression of antioxidant enzymes in rat retinal ischemia followed by reperfusion. *Metab., Clin. Exp. 55*, 892−898.
(77) Maeda, A., Crabb, J. W., and Palczewski, K. (2005) Microsomal Glutathione *S*-Transferase 1 in the Retinal Pigment Epithelium: Protection against Oxidative Stress and a Potential Role in Aging. *Biochemistry 44*, 480−489.
(78) Chida, M., Suzuki, K., Nakanishi-Ueda, T., Ueda, T., Yasuhara, H., Koide, R., and Armstrong, D. (1999) In vitro testing of antioxidants and biochemical end-points in bovine retinal tissue. *Ophthalmic Res. 31*, 407−415.
(79) Hashizume, K., Hirasawa, M., Imamura, Y., Noda, S., Shimizu, T., Shinoda, K., Kurihara, T., Noda, K., Ozawa, Y., Ishida, S., Miyake, Y., Shirasawa, T., and Tsubota, K. (2008) Retinal dysfunction and progressive retinal cell death in SOD1-deficient mice. *Am. J. Pathol. 172*, 1325−1331.

(80) Yuki, K., Ozawa, Y., Yoshida, T., Kurihara, T., Hirasawa, M., Ozeki, N., Shiba, D., Noda, K., Ishida, S., and Tsubota, K. (2011) Retinal ganglion cell loss in superoxide dismutase 1 deficiency. *Invest. Ophthalmol. Visual Sci. 52*, 4143−4150.
(81) Murphy, M. P. (2009) How mitochondria produce reactive oxygen species. *Biochem. J. 417*, 1−13.
(82) Carellia, V., Ross-Cisneros, F. N., and Sadun, A. A. (2004) Optic nerve degeneration and mitochondrial dysfunction: Genetic and acquired optic neuropathies. *Neurochem. Int. 40*, 573−584.
(83) Feher, J., Kovacs, I., Artico, M., Cavallotti, C., Papale, A., and Balacco Gabrieli, C. (2006) Mitochondrial alterations of retinal pigment epithelium in age-related macular degeneration. *Neurobiol. Aging 27*, 983−993.
(84) Sawyer, D. E., Roman, S. D., and Aitken, R. J. (2001) Relative susceptibilities of mitochondrial and nuclear DNA to damage induced by hydrogen peroxide in two mouse germ cell lines. *Redox Rep. 6*, 182−184.
(85) Chang, H. Y., and Yang, X. (2000) Proteases for cell suicide: functions and regulation of caspases. *Microbiol. Mol. Biol. Rev. 64*, 821−846.
(86) Thornberry, N. A., and Lazebnik, Y. (1998) Caspases: Enemies Within. *Science 281*, 1312−1316.
(87) Wu, J., Gorman, A., Zhou, X., Sandra, C., and Chen, E. (2002) Involvement of caspase-3 in photoreceptor cell apoptosis induced by in vivo blue light exposure. *Invest. Ophthalmol. Visual Sci. 43*, 3349−3354.
(88) O'Connor, J. C., Wallace, D. M., Colm J. O'Brien, C. J., and Cotter, T. G. (2008) A Novel Antioxidant Function for the Tumor-Suppressor Gene p53 in the Retinal Ganglion Cell. *Invest. Ophthalmol. Visual Sci. 49*, 4237−4244.
(89) Bhattacharya, S., Ray, R. M., Chaum, E., Johnson, D. A., and Johnson, L. R. (2011) Inhibition of Mdm2 sensitizes human retinal pigment epithelial cells to apoptosis. Invest. *Ophthalmol. Visual Sci. 52*, 3368−3380.
(90) Vuong, L., Conley, S. M., and Al-Ubaidi, M. R. (2012) Expression and role of p53 in the retina. *Invest. Ophthalmol. Visual Sci. 53*, 1362−1337.
(91) http://en.wikipedia.org/wiki/Golden_Eagle.
(92) Nemtzov, S. C. (2008) Uromastyx Lizards in Israel. *NDF Workship Case Studies WG 7—Reptiles and Amphibians, Case Study 5*, Mexico.
(93) Bowmaker, J. K., Heath, L. A., Wilkie, S. E., and Hunt, D. M. (1997) Visual pigments and oil droplets from six classes of photoreceptor in the retinas of birds. *Vision Res. 37*, 2183−94.
(94) Cai, J., Nelson, K. C., Wu, M., Sternberg, P., and Jones, D. P. (2000) Oxidative damage and protection of the RPE. *Prog. Retinal Eye Res. 19*, 205−221.
(95) Donovan, M., and Cotter, T. G. (2002) Caspase-independent photoreceptor apoptosis in vivo and differential expression of apoptotic protease activating factor-1 and caspase-3 during retinal development. *Cell Death Differ. 9*, 1220−1231.
(96) Bortolotti, G., Fernie, K., and Smits, J. E. (2003) Carotenoid concentration and coloration of American kestrels (*Falco sparverius*) disrupted by experimental exposure to PCBs. *Funct. Ecol. 17*, 651−657.
(97) Villafuerte, R., and Negro, J. J. (1998) Digital imaging for color measurement in ecological research. *Ecol. Lett. 1*, 151−154.
(98) Clark, W. S. (2004). Wave molt of the primaries of accipitrid raptors, and its use in ageing immatures. In *Raptors Worldwide* (Chancellor, R.D., and Meyburg, B.-U., Eds.), pp 795−804, World Working Group on Birds of Prey and Owls, Berlin, Germany.
(99) Casagrande, S., Costantini, D., Tagliavini, J., and Dell'Omo, G. (2009) Phenotypic, genetic, and environmental causes of variation in yellow skin pigmentation and serum carotenoids in Eurasian kestrel nestlings. *Ecol. Res. 24*, 273−279.
(100) Bortolotti, G. R., Tella, J. L., Forero, M. G., Dawson, R. D., and Negro, J. J. (2000) Genetics, local environment and health as factors influ-encing plasma carotenoids in wild American kestrels (*Falco sparverius*). *Proc. R. Soc. London, Ser. B 267*, 1433−1438.
(101) Costantini, D., Casagrande, S., De Filippis, S., Brambilla, G., Fanfani, A., Tagliavini, J., and Dell'Omo, G. (2006) Correlates of oxidative stress in wild kestrel nestlings (*Falco tinnunculus*). *J. Comp. Physiol., B 176*, 329−337.
(102) EL-Sayyad, H. I., Yonis, M. W. F., Bayomi, F. F. M., and Shalaby, S. (2009) Epidermal sense organs of the Gekkonid tropicolotes tripolitanus Peters 1880. *J. Cell Anim. Biol. 3*, 088−092.
(103) Wilm, T. M., Bohme, H., Wagner, P., Lutzmann, N., and Andreas Schmitz, A. (2007) On the Phylogeny and Taxonomy of the Genus *Uromastyx* Merrem, 1820 (Reptilia: Squamata: Agamidae: Uromastycinae) − Resurrection of the Genus *Saara* Gray, 1845. *Bonner Zool. Beitr. 56*, 55−99.
(104) Gilberstadt, M. L., and Russell, J. A. (1984) Determination of picomole quantities of acetylcholine and choline in physiologic salt solutions. *Anal. Biochem. 138*, 78−85.
(105) Schlumpf, M., Lichtensteiger, W., Langemann, H., Waser, P. G., and Hefti, F. A. (1973) A Fluorometric micromethod for the simultaneous de-termination of serotonin, noradrenaline and dopamine in milli gram amounts of brain tissue. *Biochem. Pharmacol. 23*, 2437−2446.
(106) Heinrikson, R. L., and Meredith, S. C. (1984) Amino acid analysis by reverse-phase high-performance liquid chromatography: precolumn derivatization with phenylisothiocyanate. *Anal. Biochem. 136*, 65−74.
(107) Bock, P. P., Kramer, R., and Pavelka, M. (1980) Peroxisomes and related particles. In *Cell Biology Monographs*, Vol. 7, pp 44−74, Springer, Berlin.
(108) Habig, H., Pabst, J. H., and Jakoby, W. B. (1974) Glutathione-S- transferase. The first enzymes step in mercapturic and formation. *J. Biol. Chem. 249*, 7130−7139.
(109) Niskikimi, M., Rao, N. A., and Yagii, K. (1972) The occurence of superoxide anion in there action of reduced phenazine methosulfate and molecular oxygen. *Biochem. Biophys. Res. Commun. 46*, 849−854.
(110) Ohkawa, H., Ohishi, N., and Yagi, K. (1979) Assay for lipid peroxides in animal tissues by thiobarbituric acid reaction. *Anal. Biochem. 95*, 351−358.